# Aerodynamic Efforts of Propellers at high incidence angles with 3D URANS Computation

Akshay Anand[1]
Master Student in Aeronautics and Space, Track: Turbulence

**Supervisor:**
**Thierry JARDIN** [2]
Department of Aerodynamics, Energetics
and Propulsion, ISAE - SUPAERO
Toulouse , France

March 2019 to September 2019

# Contents

# Unmanned Aerial Vehicle

- It is an aircraft without a pilot on-board, hence the name is called Unmanned aerial vehicle, also referred as DRONE
- Multi-rotor : generates lift via rotary wings
- Fixed wing : predetermined airfoil which makes UAV able to generate lift


1


2


3

1. Quadcopter
2. Hexacopter
3. Fixed Wing UAV

# What is Vertical take-off and Landing ?

- An aircraft that can hover, take-off and land vertically
- VTOL can take-off and land at any worst conditions
- No need of runway
- Best examples Helicopters and Drones

# What is Vertical take-off and Landing ?

- An aircraft that can hover, take-off and land vertically
- VTOL can take-off and land at any worst conditions
- No need of runway
- Best examples Helicopters and Drones

# What is Vertical take-off and Landing ?

- An aircraft that can hover, take-off and land vertically
- VTOL can take-off and land at any worst conditions
- No need of runway
- Best examples Helicopters and Drones

# Applications of UAV

- Aerospace
- Military
- Cargo Transport
- Aerial Surveillance



# Motivation

- Major challenge with UAV development is to achieve good handling characteristics between hover and horizontal flight
- VTOL needs a stable transition between take-off and horizontal flight.
- Aerodynamics of propeller is the key parameter.

# Transition from near- hover to horizontal cruise condition

- Flight parameters like AoA, airspeed vary drastically
- Airflow can't be considered axisymmetric for propeller
- Propellers at 0 deg incidence angle is considered as axisymmetric

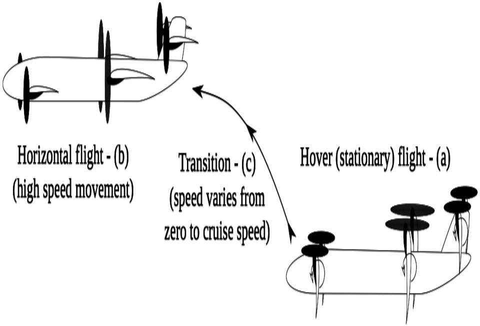


a

a. Airimitoaie et al, ICMM, 2018

# Literature Review

- Leng et al [4] studied aerodynamics of rotors at high incidence angle for various advance ratio and blade pitch angles.
  - Experiment catches attention of 3D effects such as stall-delay.

- Theys et al [5] conducted experiments about VTOL of MAV, they measured aerodynamics of rotors at high incidence angles between 0 deg to 180 deg
  - However, this experiment is adopted to a rotor having an airfoil which lacks detailed 2D aerodynamic data.

4. Experimental analysis of propeller forces and moments at high incidence angles, AIAA, 2019

5. Wind tunnel testing of VTOL, MAV propeller in tilting operating mode, ICUAS, 2014

# Literature Review

- Leng et al [4] studied aerodynamics of rotors at high incidence angle for various advance ratio and blade pitch angles.
  - Experiment catches attention of 3D effects such as stall-delay.
- Theys et al [5] conducted experiments about VTOL of MAV, they measured aerodynamics of rotors at high incidence angles between 0 deg to 180 deg
  - However, this experiment is adopted to a rotor having an airfoil which lacks detailed 2D aerodynamic data.

4. Experimental analysis of propeller forces and moments at high incidence angles, AIAA, 2019
5. Wind tunnel testing of VTOL, MAV propeller in tilting operating mode, ICUAS, 2014

# Literature Review

1. Several researcher used numerical methods to understand aerodynamics of propellers at high incidence angles.
2. Researches employed 3D CFD to solve URANS equation as it is less costly compared to DNS/LES/DES

- Smith et al [6] evaluated 4 distinct turbulence models to calculate aerodynamic coefficients of airfoil.
- Abras et al [7] calculated aerodynamics of tilt rotor aircraft, used Spallart-Allamaras Model with two CFD code OVERFLOW 2.1 & FUND 10.8
- Welch et al [8] studied performance of tilt rotor at take-off, 15000 rpm, 38 to 54 deg incidence angle used Baldwin Lomax and K-Omega

6. Evaluation of CFD to determine 2D airfoil characteristics, AHS, 2006
7. Analysis of CFD modeling techniques over the MV-22 tiltrotor, 2010
8. Computational Study of the impact of unsteadiness on the aerodynamic

# Literature Review

1. Several researcher used numerical methods to understand aerodynamics of propellers at high incidence angles.
2. Researches employed 3D CFD to solve URANS equation as it is less costly compared to DNS/LES/DES

- Smith et al [6] evaluated 4 distinct turbulence models to calculate aerodynamic coefficients of airfoil.
- Abras et al [7] calculated aerodynamics of tilt rotor aircraft, used Spallart-Allamaras Model with two CFD code OVERFLOW 2.1 & FUND 10.8
- Welch et al [8] studied performance of tilt rotor at take-off, 15000 rpm, 38 to 54 deg incidence angle used Baldwin Lomax and K-Omega

6. Evaluation of CFD to determine 2D airfoil characteristics, AHS, 2006
7. Analysis of CFD modeling techniques over the MV-22 tiltrotor, 2010
8. Computational Study of the impact of unsteadiness on the aerodynamic

# Literature Review

1. Several researcher used numerical methods to understand aerodynamics of propellers at high incidence angles.
2. Researches employed 3D CFD to solve URANS equation as it is less costly compared to DNS/LES/DES

- Smith et al[6] evaluated 4 distinct turbulence models to calculate aerodynamic coefficients of airfoil.
- Abras et al[7] calculated aerodynamics of tilt rotor aircraft, used Spallart-Allamaras Model with two CFD code OVERFLOW 2.1 & FUND 10.8
- Welch et al[8] studied performance of tilt rotor at take-off, 15000 rpm, 38 to 54 deg incidence angle used Baldwin Lomax and K-Omega

6. Evaluation of CFD to determine 2D airfoil characteristics, AHS, 2006
7. Analysis of CFD modeling techniques over the MV-22 tiltrotor, 2010
8. Computational Study of the impact of unsteadiness on the aerodynamic

# Approach

1. Experiments posses certain limitations, for instance it is inefficient to obtain data at different rotor geometries.
2. Difficult to find experimental data containing detailed flow structure, load distributions.

- We implemented CFD to analyze aerodynamics of rotors at high incidence angle.
- Applied URANS and calculated results are compared with experimental data to validate the computation.

**To understand precisely aerodynamics of rotors**

Need to understand the flow condition in the blade section of rotors at high incidence angles

# Approach

1. Experiments posses certain limitations, for instance it is inefficient to obtain data at different rotor geometries.
2. Difficult to find experimental data containing detailed flow structure, load distributions.

- We implemented CFD to analyze aerodynamics of rotors at high incidence angle.
- Applied URANS and calculated results are compared with experimental data to validate the computation.

**To understand precisely aerodynamics of rotors**

Need to understand the flow condition in the blade section of rotors at high incidence angles

# Propellers at non-zero incidence angles

- Subjected to asymmetrical forces and moments in the propeller plane.
- When the tangential component of free stream is opposite in direction to the rotational velocity it is called advancing side of propeller
- Exist difference between advancing and retreating side

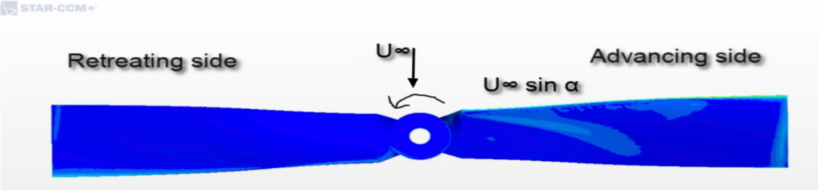

# Velocity Diagram

- Imagine we have a propeller and we cut into halves
- We look at the radial direction
- Propellers at 0 deg incidence is considered as axisymmetric
- J is proportional to

$$J = \frac{U_\infty \cos\alpha}{nD}$$

- J determines how fast blade is rotating w.r.t $U_\infty$

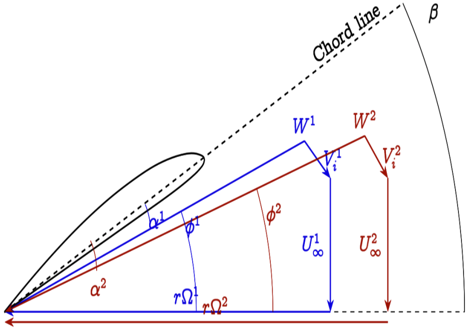

# Velocity Diagram

- Imagine we have a propeller and we cut into halves
- We look at the radial direction
- Propellers at 0 deg incidence is considered as axisymmetric
- J is proportional to

$$\mathbf{J} = \frac{U_\infty \cos\alpha}{nD}$$

- J determines how fast blade is rotating w.r.t $U_\infty$

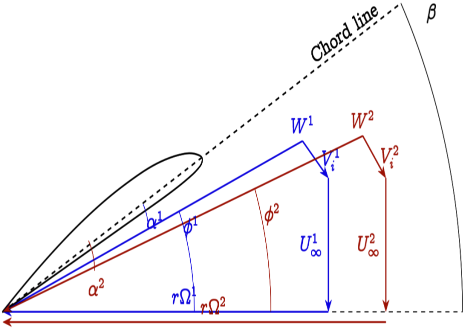

# Velocity Diagram

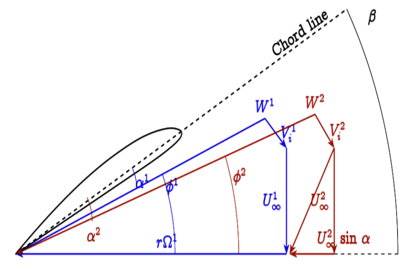


Advancing Side

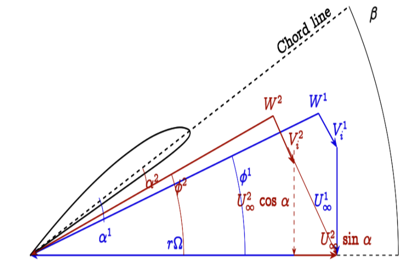


Retreating Side

- Relative wind magnitude and AoA depends on $r\Omega$, $U_\infty$ & $V_i$
- $U_\infty$ can have both tangential and axial component depending on incidence angle
- Larger relative wind magnitude and AoA at advancing side as tangential component of $U_\infty$ and $r\Omega$ are in opposite direction

# URANS Equations

- Several ways to solve turbulent flows, DNS/LES/DES/URANS
- URANS is cheaper in terms of computational cost and time & gives credible result for large scale periodicity and Vortex sheeding.
- URANS starts with following Navier Stoke's equation for incompressible flow

$$\frac{\partial u_i}{\partial x_i} = 0 \tag{1}$$

$$\frac{\partial u_i}{\partial t} + u_j \frac{\partial u_i}{\partial x_j} = f_i - \frac{1}{\rho}\frac{\partial p}{\partial x_i} + v \frac{\partial^2 u_i}{\partial x_j \partial x_j} \tag{2}$$

$$u(x,t) = \overline{u}(x) + u'(x,t) \tag{3}$$

# URANS Equations

Applying Reynolds averaging and separating the terms related to turbulence fluctuation and average velocity

$$\frac{\partial \overline{u}_t}{\partial x_i} = 0 \tag{4}$$

$$\frac{\partial \overline{u}_t}{\partial t} + \overline{u}_j \frac{\partial \overline{u}_t}{\partial x_j} + u'_j \frac{\partial u'_t}{\partial x_j} = \overline{f}_t - \frac{1}{\rho}\frac{\partial \overline{p}}{\partial x_i} + v \frac{\partial^2 \overline{u}_t}{\partial x_j \partial x_j} \tag{5}$$

Arranging the equation to left to have Reynolds stress term,

$$\rho \frac{\partial \overline{u}_i}{\partial t} + \rho \overline{u}_j \frac{\partial \overline{u}_i}{\partial x_j} = \rho \overline{f}_i + \frac{\partial}{\partial x_j} - \overline{p}\delta_{ij} + 2\mu \overline{S}_{ij} - \rho \overline{u'_i u'_j}$$

$$\overline{S}_{ij} = \frac{1}{2}\left(\frac{\partial \overline{u}_i}{\partial x_j} + \frac{\partial \overline{u}_j}{\partial x_i}\right)$$

# URANS Equations

Applying Reynolds averaging and separating the terms related to turbulence fluctuation and average velocity

$$\frac{\partial \overline{u}_t}{\partial x_i} = 0 \tag{4}$$

$$\frac{\partial \overline{u}_t}{\partial t} + \overline{u}_j \frac{\partial \overline{u}_t}{\partial x_j} + u'_j \frac{\partial u'_t}{\partial x_j} = \overline{f}_t - \frac{1}{\rho}\frac{\partial \overline{p}}{\partial x_i} + v\frac{\partial^2 \overline{u}_t}{\partial x_j \partial x_j} \tag{5}$$

Arranging the equation to left to have Reynolds stress term,

$$\rho\frac{\partial \overline{u}_i}{\partial t} + \rho\overline{u}_j \frac{\partial \overline{u}_i}{\partial x_j} = \rho\overline{f}_i + \frac{\partial}{\partial x_j} - \overline{p}\delta_{ij} + 2\mu\overline{S_{ij}} - \boxed{\rho\overline{u'_i u'_j}}$$

$$\overline{S}_{ij} = \frac{1}{2}\left(\frac{\partial \overline{u}_i}{\partial x_j} + \frac{\partial \overline{u}_j}{\partial x_i}\right) \tag{6}$$

# URANS Equation

URANS is applicable for flow having large scale periodicity.

- Rotation of Propellers
- Vortex sheeding

Here, URANS is function of space(x) and time (t), so we perform ensemble average, not the time average :

$$\rho \frac{\partial \overline{u}_i}{\partial t} + \rho \overline{u}_j \frac{\partial \overline{u}_i}{\partial x_j} = \rho \overline{f}_i + \frac{\partial}{\partial x_j}\left[-\overline{p}\delta_{ij} + 2\mu \overline{S_{ij}} - \rho \overline{u_i' u_j'}\right] \quad (7)$$

When there exist deterministic unsteadiness, turbulence model represent fluctuation relative to ensemble average [a]

a. Durbin et al, AIAA,2019

# URANS Equation

URANS is applicable for flow having large scale periodicity.

- Rotation of Propellers
- Vortex sheeding

Here, URANS is function of space(x) and time (t), so we perform ensemble average, not the time average :

$$\rho\frac{\partial \overline{u}_i}{\partial t} + \rho\overline{u}_j\frac{\partial \overline{u}_i}{\partial x_j} = \rho\overline{f}_i + \frac{\partial}{\partial x_j}\left[-\overline{p}\delta_{ij} + 2\mu\overline{S_{ij}} - \rho\overline{u_i' u_j'}\right] \tag{7}$$

When there exist deterministic unsteadiness, turbulence model represent fluctuation relative to ensemble average [a]

a. Durbin et al, AIAA,2019

# Computational domain

Computational domain is divided into 2 regions :

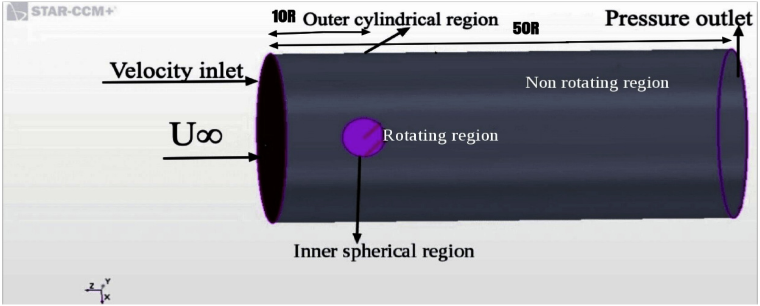


Using Sliding Mesh entire inner domain can be tilted at angle of incidence w.r.t free stream velocity, and could be rotated at given rps relative to stationary outer domain

Rotating and non-rotating region are joined by internal interface

# Computational domain

Computational domain is divided into 2 regions :

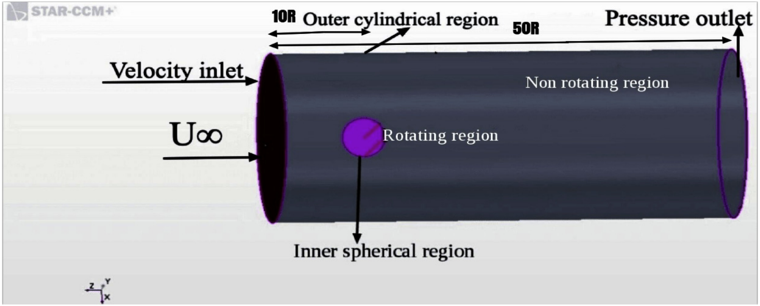


Using Sliding Mesh entire inner domain can be tilted at angle of incidence w.r.t free stream velocity, and could be rotated at given rps relative to stationary outer domain

Rotating and non-rotating region are joined by internal interface

# Mesh

The radius of cylindrical wall is 10R which is large enough to remove the effect of cylindrical wall on aerodynamic efforts of propeller.

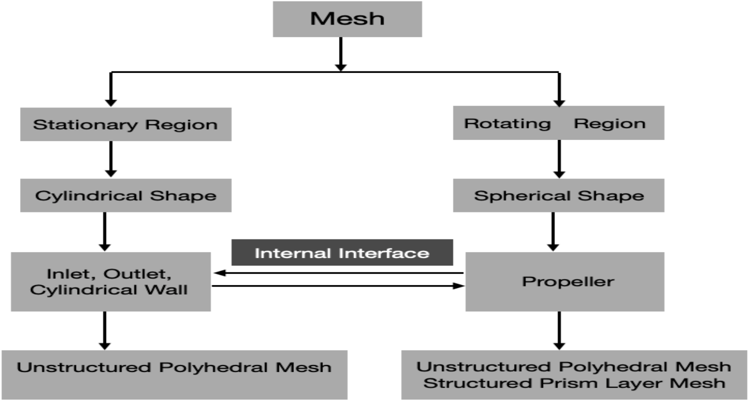

# Mesh

Unstructured Mesh

Structured Prism Layer

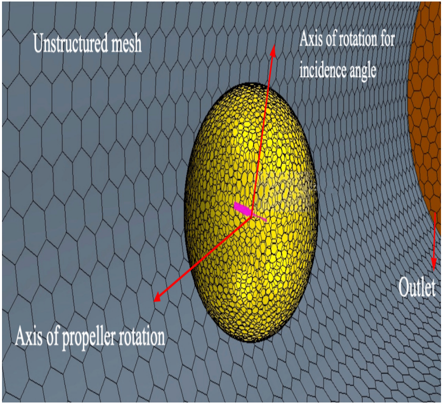


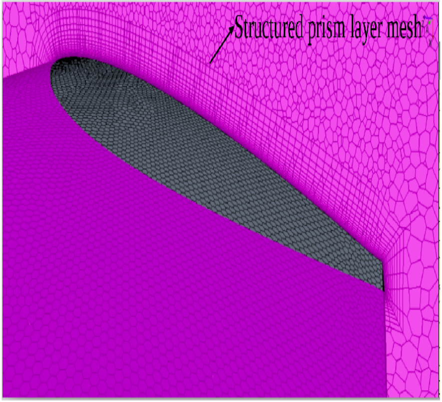


SUPAERO

# Prism Layer Mesh

- Prism layer is optimized to solve boundary layer flow.
- BL (Boundary Layer) is located at the immediate vicinity of rotor surface, where viscosity dominates the flow physics.
- Two parameters are needed to define prism layer thickness

1. Total thickness : In this research it is calculated as 1.166mm
2. First cell height : should be located appropriately inside TBL, need to understand y+
   - Y+ is a non-dimensional number that explains the proximity to wall boundary
   - Low y+ bottom of boundary layer, high y+ top of BL, as a consequence of no-slip velocity is zero at wall
   - In this work y+ = 1 as we used low y+ turbulence model (Spallart-Allamaras) after comparison with K-epsilon

# Prism Layer Mesh

- Prism layer is optimized to solve boundary layer flow.
- BL (Boundary Layer) is located at the immediate vicinity of rotor surface, where viscosity dominates the flow physics.
- Two parameters are needed to define prism layer thickness

1. Total thickness : In this research it is calculated as 1.166mm
2. First cell height : should be located appropriately inside TBL, need to understand y+
   - Y+ is a non-dimensional number that explains the proximity to wall boundary
   - Low y+ bottom of boundary layer, high y+ top of BL, as a consequence of no-slip velocity is zero at wall
   - In this work y+ = 1 as we used low y+ turbulence model (Spallart-Allamaras) after comparison with K-epsilon

# Prism Layer Mesh

- Prism layer is optimized to solve boundary layer flow.
- BL (Boundary Layer) is located at the immediate vicinity of rotor surface, where viscosity dominates the flow physics.
- Two parameters are needed to define prism layer thickness

1. Total thickness : In this research it is calculated as 1.166mm
2. First cell height : should be located appropriately inside TBL, need to understand y+
   - Y+ is a non-dimensional number that explains the proximity to wall boundary
   - Low y+ bottom of boundary layer, high y+ top of BL, as a consequence of no-slip velocity is zero at wall
   - In this work y+ = 1 as we used low y+ turbulence model (Spallart-Allamaras) after comparison with K-epsilon

# Solver Description & Turbulence Models

- Segregated solver is used which decouples velocity and pressure by solving NSE for incompressible flow
- Second order implicit iteration method is used for both spatial and temporal discritization
- Each time step contains 20 sub iterations to improve the convergence of URANS computation
- Spallart Allamaras turbulence model gives an error of 6% in $\mathbf{C_T}$ and K-epsilon 13% in $\mathbf{C_T}$ when compared with experimental data

# Mesh Convergence Study

- Mesh Convergence is the test to find optimum number of mesh for computation
- Fine mesh improved results but costs huge computation cost & time

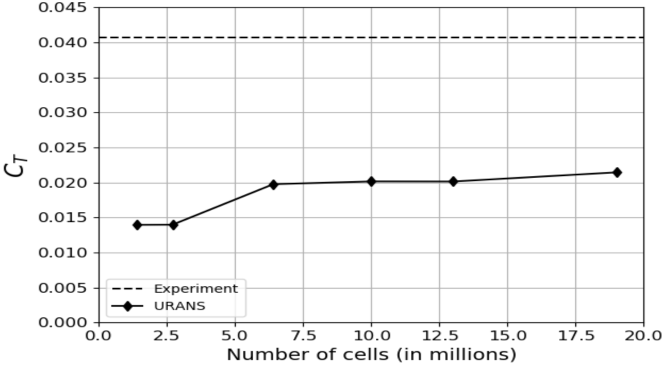

# Mesh Convergence Study

- Mesh Convergence is the test to find optimum number of mesh for computation
- Fine mesh improved results but costs huge computation cost & time

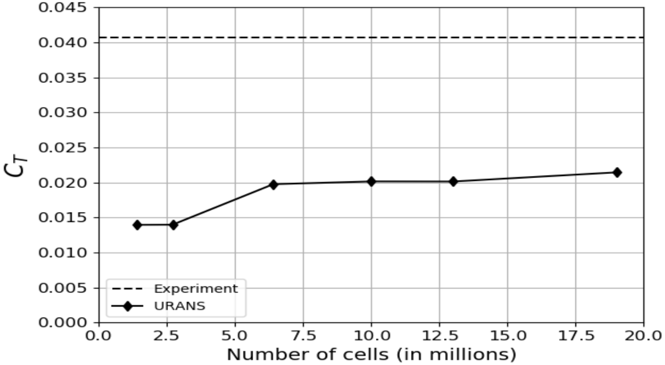

# Mesh Convergence Study

Asymptotic trend is found around cell size close to 6.4 millions

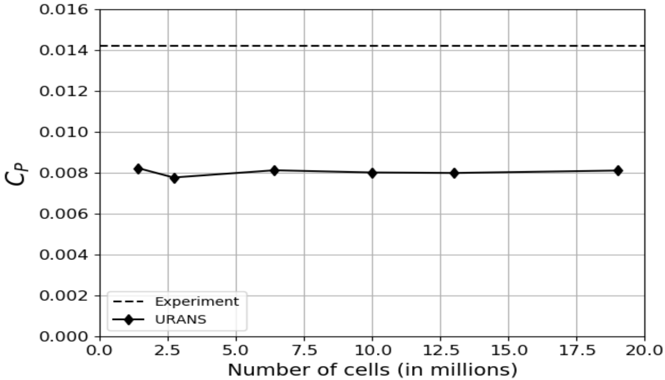


Total number of cells is around 6.4 millions

# Mesh Convergence Study

Asymptotic trend is found around cell size close to 6.4 millions

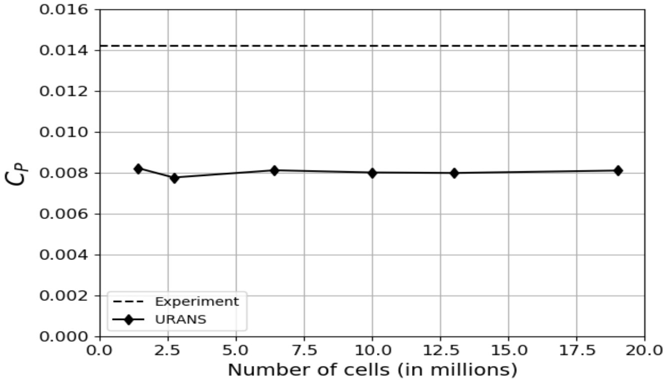


Total number of cells is around 6.4 millions

# Mesh Convergence Study

| No. of Cells (Millions) | Surface Size | $C_T$ (URANS) | $C_P$ (URANS) |
|---|---|---|---|
| 1.4 | 5.0E-04 | 0.013934 | 0.008237 |
| 2.7 | 3.75E-04 | 0.013954 | 0.007778 |
| 6.4 | 2.5E-04 | 0.019739 | 0.008131 |
| 10 | 2.0E-04 | 0.020137 | 0.008023 |
| 13 | 1.75E-04 | 0.020123 | 0.007999 |
| 19 | 1.5E-04 | 0.021427 | 0.008119 |

TABLE – Surface size and there corresponding aerodynamic coefficients at J =1

# Time Evolution Plot

After 6th rotation, the initial transient has decayed & similar trend for all the configuration of grid size

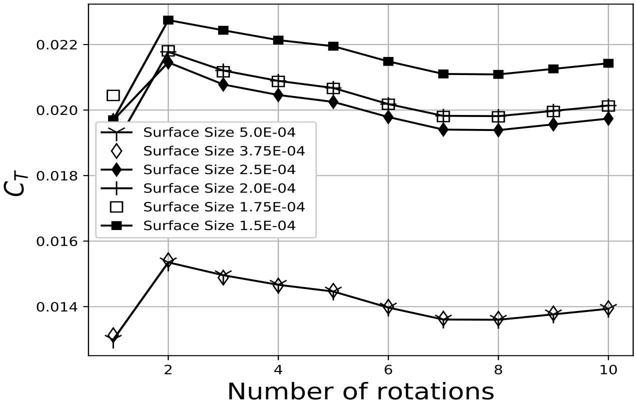

# Axisymmetric case

- J is varied from 0.19 to 0.93 at 0 deg incidence angle
- URANS aims to understand the effect of rotational velocity on URANS calculation of rotor.

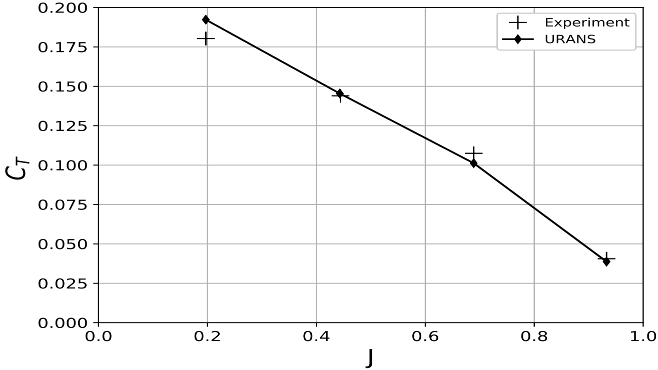

# Axisymmetric case

- J is varied from 0.19 to 0.93 at 0 deg incidence angle
- URANS aims to understand the effect of rotational velocity on URANS calculation of rotor.

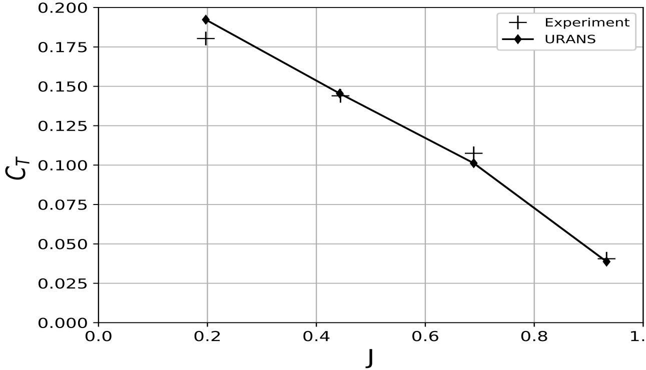

# Axisymmetric case

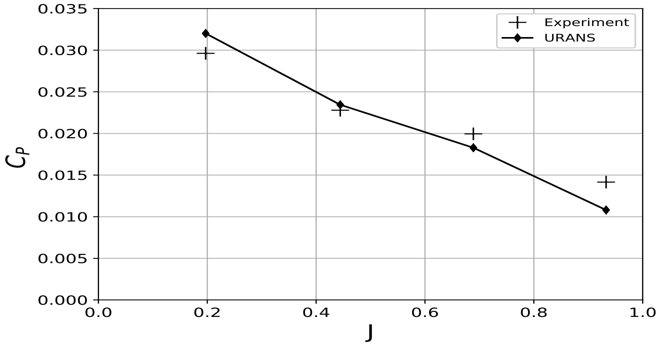


- A slight difference between experimental and URANS
- Drag is more affected by laminar to turbulent flow transition, and is more complicated to be exactly predicted by URANS.

# Asymmetric Case

- URANS simulations are performed at high incidence angles $\alpha_p$ from 0 deg to 90 deg at different J.
- URANS aims to understand the effect of incidence angle on the URANS simulation of rotors.

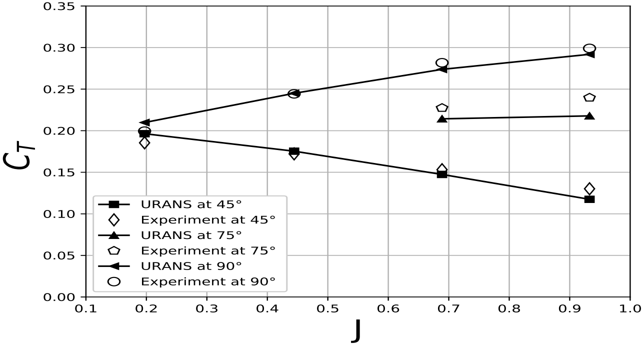

# Asymmetric Case

- URANS simulations are performed at high incidence angles $\alpha_p$ from 0 deg to 90 deg at different J.
- URANS aims to understand the effect of incidence angle on the URANS simulation of rotors.

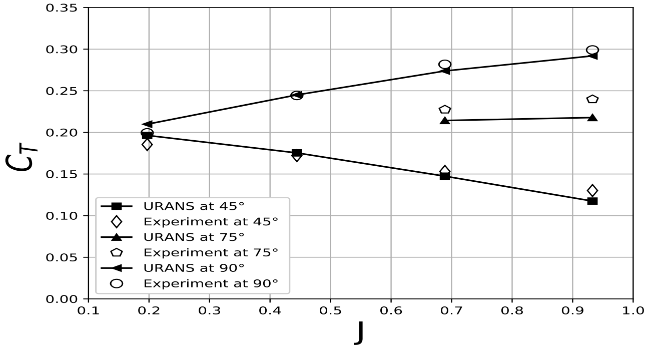

# Asymmetric Case

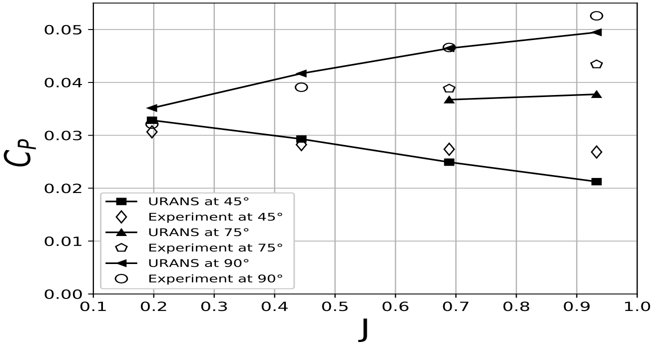


- Influence of J depend on incidence angle
- At 45 deg $C_T$ & $C_P$ decreases
- At incidence angle 75 deg there is a dividing point
- Non linear growth at higher incidence angle

# Asymmetric Case

## Normal Force

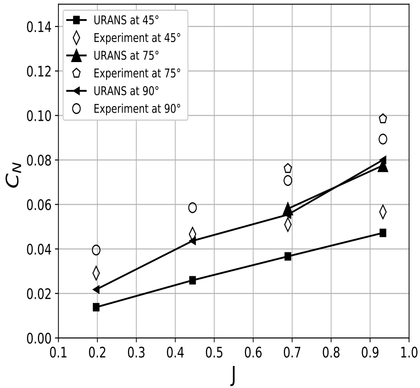


## Yaw Moment

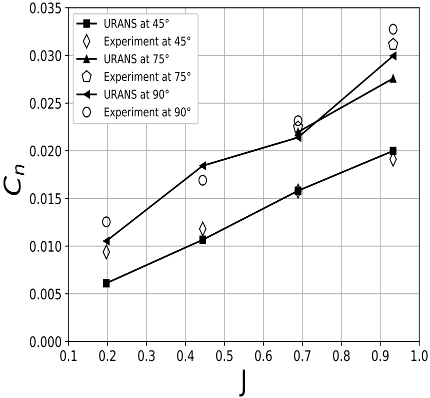

# Asymmetric Case

- Thrust coefficient from URANS varies from experiment with an error of atmost 10%
- Power coefficient from URANS varies with an error of around 12 % at different incidence angle
- Normal force depends on the stability
- Yaw moment shows quasi-linear growth with respect to advance ratio
- The error reported in yaw moment is around 15-19%

# Asymmetric Case

- Thrust coefficient from URANS varies from experiment with an error of atmost 10%
- Power coefficient from URANS varies with an error of around 12 % at different incidence angle
- Normal force depends on the stability
- Yaw moment shows quasi-linear growth with respect to advance ratio
- The error reported in yaw moment is around 15-19%

# Asymmetric Case

- Thrust coefficient from URANS varies from experiment with an error of atmost 10%
- Power coefficient from URANS varies with an error of around 12 % at different incidence angle
- Normal force depends on the stability
- Yaw moment shows quasi-linear growth with respect to advance ratio
- The error reported in yaw moment is around 15-19%

# Flow Visualisation

- Flow structure is visualised in terms of isosurface with constant Q-Criterion (Q = 50,000)
- It identifies the region where rotation dominates shear.

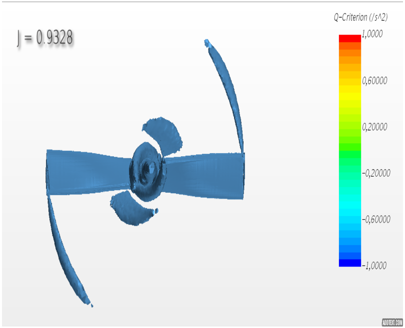


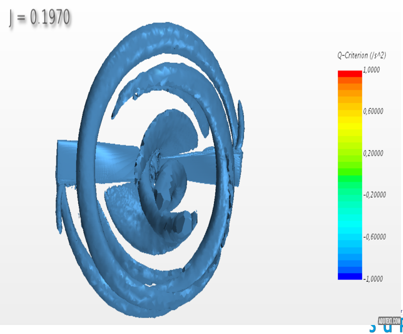

# Flow Visualisation

- No strong flow separation at higher J as relative wind AoA at each airfoil element is lower then critical stall angle of NACA0012 series airfoil.
- Critical stall angle for NACA0012 airfoil is 8 deg and it depends on Re and airfoil thickness
- At J = 0.19 with 0 deg IA there exist both leading and trailing edge separations because for low J, the relative wind angle of attack exceeds the critical stall angle of NACA0012 series airfoil.
- In some regions there is absence of separation and this could be because of maximum rotational effect near the roots of rotors.
- Less complexity at higher J, hence URANS gives accurate result at higher J compared to lower J

# Flow Visualisation

- No strong flow separation at higher J as relative wind AoA at each airfoil element is lower then critical stall angle of NACA0012 series airfoil.
- Critical stall angle for NACA0012 airfoil is 8 deg and it depends on Re and airfoil thickness
- At J = 0.19 with 0 deg IA there exist both leading and trailing edge separations because for low J, the relative wind angle of attack exceeds the critical stall angle of NACA0012 series airfoil.
- In some regions there is absence of separation and this could be because of maximum rotational effect near the roots of rotors.
- Less complexity at higher J, hence URANS gives accurate result at higher J compared to lower J

# Flow Visualisation

- No strong flow separation at higher J as relative wind AoA at each airfoil element is lower then critical stall angle of NACA0012 series airfoil.
- Critical stall angle for NACA0012 airfoil is 8 deg and it depends on Re and airfoil thickness
- At J = 0.19 with 0 deg IA there exist both leading and trailing edge separations because for low J, the relative wind angle of attack exceeds the critical stall angle of NACA0012 series airfoil.
- In some regions there is absence of separation and this could be because of maximum rotational effect near the roots of rotors.
- Less complexity at higher J, hence URANS gives accurate result at higher J compared to lower J

# Flow Visualisation

Flow Visualisation at higher J at 45 deg IA has been performed

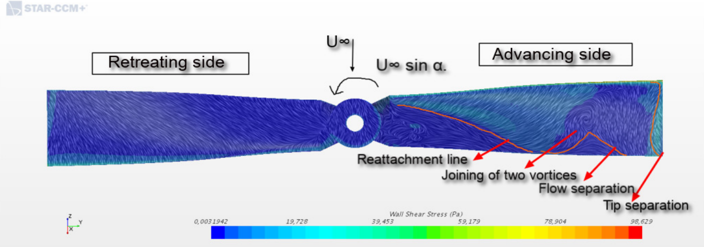


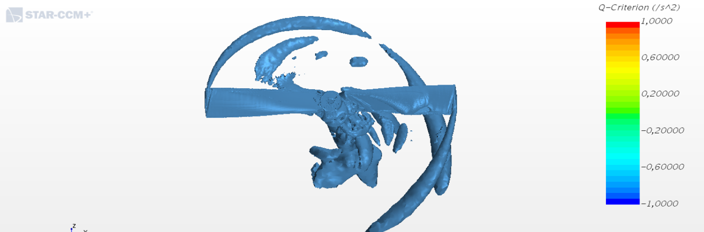

# Conclusion and Future work

- At 0 degree IA, J is varied to understand effect of rotational speed, good results for $C_T$, but not for $C_P$ as drag is affected by laminar to turbulent transition and is difficult to predict by URANS
- Higher accuracy at greater J as flow structure are more stable
- Low J needs stable aerodynamic coefficient during transition phase, it could be interpreted that low J are more appropriate to the transition flights.
- Low J at 0 deg incidence angle, there exists vortex sheeding near the tip of the blade and vortex near hub seems to be stable, this is because of rotational effects

- At high IA, there exists attached and stable flow at the retreating side but there is a vortex sheeding at the advancing side because it has larger AoA then retreating side

  Future work

  Research is needed to be done to find a stable aerodynamic coefficients during transition phase

# Acknowledgement

- Thanks to Dr. Thierry JARDIN for his supervision.
- Special thanks to Mr. Nicolas Doue, Yuchen Leng and members of DAEP at ISAE-SUPAERO, Toulouse
- Thanks to SUPAERO for the computational resources
- Thanks to Dr. Florent Margnat for his guidance as a academic supervisor in the project during the last 6 months

Questions